Organic & Biomolecular Chemistry

PAPER

View Article Online
View Journal | View Issue

Cite this: *Org. Biomol. Chem.*, 2014, **12**, 7045

Novel EDTA-ligands containing an integral perylene bisimide (PBI) core as an optical reporter unit†

Mario Marcia,[a] Prabhpreet Singh,[b] Frank Hauke,[a] Michele Maggini[c] and Andreas Hirsch*[a]

Received 15th May 2014,
Accepted 10th July 2014

DOI: 10.1039/c4ob01007h

www.rsc.org/obc

The synthesis, characterization and metal complexation of a new class of perylene bisimides (PBIs) as an integral part of ethylenediaminetetraacetic acid (EDTA) are reported. The simplest representative, namely derivative **1a**, was synthesized both by a convergent as well as a direct approach while the elongated derivatives, **1b** and **1c**, were obtained only *via* a convergent synthetic pathway. All these new prototypes of water-soluble perylenes are bolaamphiphiles and were fully characterized by ^{1}H- and ^{13}C-NMR spectroscopy, matrix assisted laser desorption ionization-time of flight (MALDI-TOF) mass spectrometry and IR spectroscopy. In order to acquaint ourselves with the behaviour in solution of our PBIs bearing dendritic wedges, the simplest derivative, **1a**, was chosen and tested by means of UV/Vis and fluorescence spectroscopy as well as by zeta-potential measurements. A photoexcitation induced intramolecular photo-electron transfer (PET) can be observed in these molecules. Therefore their potential applications as sensors can be imagined. Model compound **1a** efficiently coordinates trivalent metal cations both in water and dimethyl sulfoxide (DMSO). Significantly, the effects of the complexation strongly depend on the aggregation state of the PBI molecules in solution. As a matter of fact, in water, the presence of M^{3+} ions triggers the formation of light emitting supramolecular aggregates (excimers). On the other hand, in DMSO-rich solutions metal complexation leads to the suppression of the PET and leads to a strong fluorescence enhancement.

Introduction

Perylene bisimides (PBIs) represent a class of aromatic chromophores with a series of interesting properties. From an industrial point of view they find widespread applications as high-performance pigments[1] due to their fascinating opto-electronic and electrochemical properties.[2] Therefore, they represent integral components in photovoltaic devices,[3] sensors,[4] OLEDs,[5] OFETs[6] as well as dye-lasers[7] and have been used as building blocks for liquid crystals,[8,9] for membrane labelling[10] and in photodynamic therapy.[11]

PBIs are usually insoluble in water. Therefore, several attempts have been performed in order to increase their solubility in aqueous media, either with functionalization in the bay region[12–16] or at the side imide groups.[17–25] Recently, we have introduced a series of highly water-soluble PBIs containing anionic ($\mathbf{R^1}$) or cationic ($\mathbf{R^2}$) Newkome dendronized substituents – representative examples are given in Fig. 1. Their aggregation behavior dependent on the pH value, ionic strength and concentration[26–28] has been investigated and based on their pronounced solubility, their ability to exfoliate and stabilize single walled carbon nanotubes (SWCNTs)[29] and graphene in water[30,31] has been demonstrated.

Here, we report the synthesis, characterization and properties of a new family of PBI-based amphiphiles. These derivatives belong to a novel class of PBI-based surfactants, where di- and polyamine spacers have been used as building blocks for the construction of arrays of oligocarboxylic acid molecules. They can be regarded as elongated ethylenediaminetetraacetic acid (EDTA) ligands containing an integral aromatic perylene bisimide (PBI) core as an optical reporter unit.

In addition, these EDTA-PBIs (Fig. 2) are characterized by a very small periphery in comparison with the Newkome dendro-

[a]*Department of Chemistry and Pharmacy and Institute of Advanced Materials and Processes (ZMP), Friedrich-Alexander University Erlangen – Nürnberg, Henkestrasse 42, 91054 Erlangen, Germany. E-mail: andreas.hirsch@fau.de; Fax: (+49)9131-8526864*

[b]*Department of Chemistry, UGC Centre for Advanced Studies, Guru Nanak Dev University, Amritsar 143005, India*

[c]*Department of Chemical Sciences, University of Padua, Via Marzolo 1, 35126 Padua, Italy*

†Electronic supplementary information (ESI) available. See DOI: 10.1039/c4ob01007h

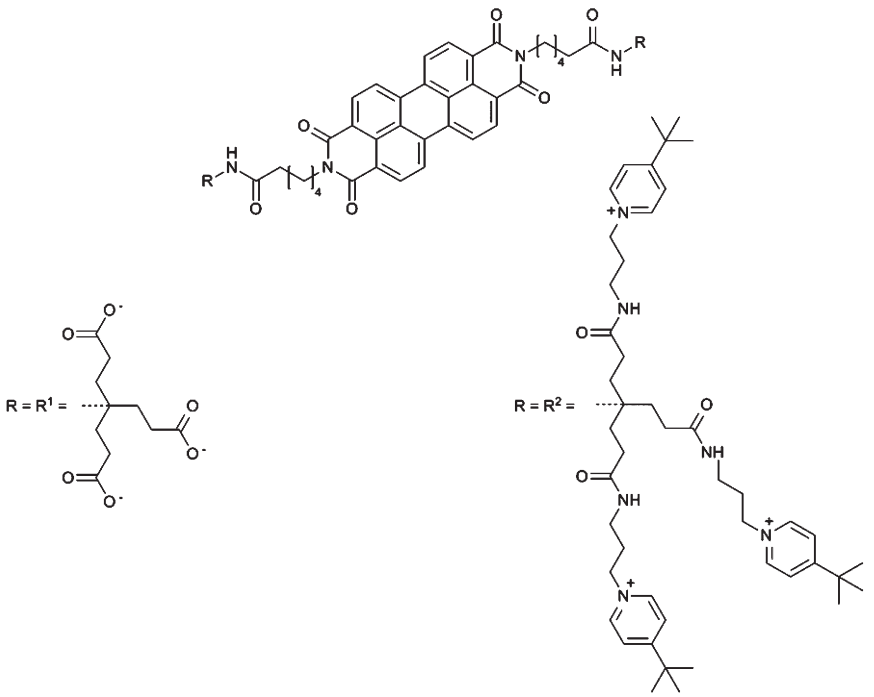

Fig. 1 Structure of 1st generation Newkome dendronized PBIs.

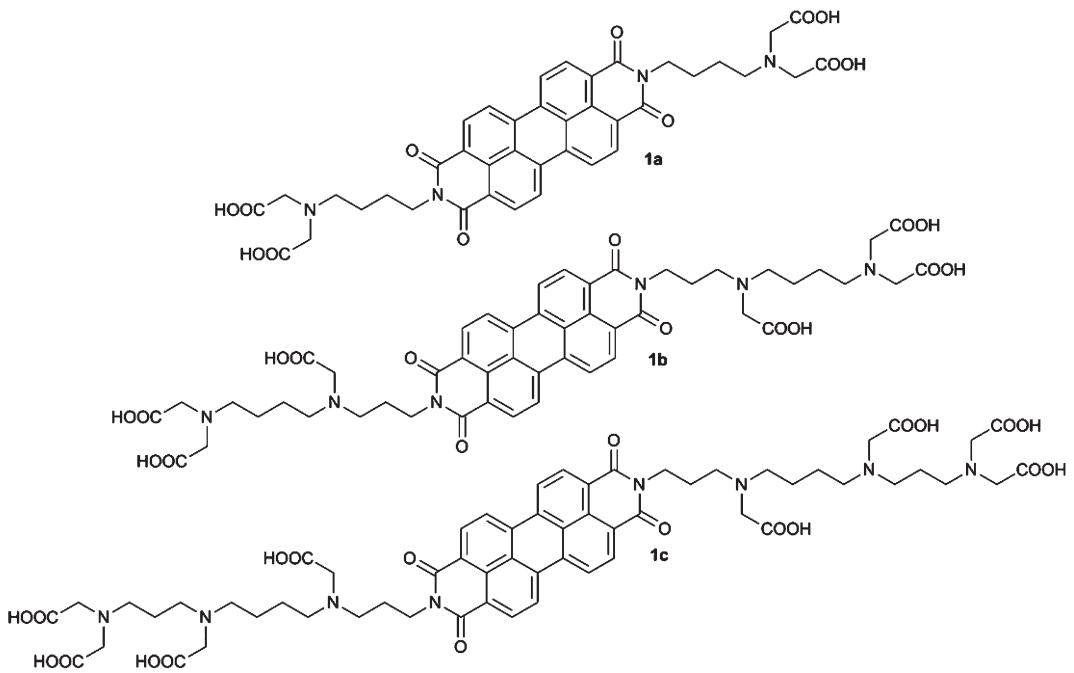

Fig. 2 Structure of EDTA-PBIs, **1a–c**.

nized ones (Fig. 1). The presence of big bulky substituents at both termini of the PBI is expected to strongly determine their aggregation behavior in solution, leading to the formation of monomers even at high concentrations. Although this feature is generally desirable, it could be a hurdle in certain specific applications, such as the dispersion/exfoliation of carbon allotropes where strong aggregation of the exfoliating agent is generally pursued[32] in order to optimise the production of individualized graphene layers/carbon nanotubes in solution. Therefore, smaller side groups emphasize the importance of the molecular core, still ensuring good water solubility and offering supplementary chelation properties. Moreover, the

terminal units of PBIs **1a–c** provide an additional feature as they enable a facile metal-chelation ability in both aqueous and organic solutions. Due to the presence of the PBI core as an optical reporter unit, the complexation of various metal cations can be studied easily by means of optical analytical techniques, such as UV/Vis and fluorescence spectroscopy.

Results and discussion

For the synthesis of **1a**, two different chemical strategies were pursued. The first route (Scheme 1, top) is based on a classical convergent synthetic approach, where the selectively functionalized protected amine **2** was condensed with perylene-3,4,9,10-tetracarboxylic dianhydride (PTCDA), yielding the *tert*-butyl protected version **3**, which was subsequently deprotected in trifluoroacetic acid (TFA) – for further details regarding the synthesis of compound **2** see ESI.† The free acid **1a** is obtained with an overall yield of 21.6% (based on the starting material putrescine). In addition, this approach is quite time consuming and employs several selective protection and deprotection steps, which impede a straightforward scale-up of the synthesis.

The second strategy (Scheme 1, bottom) involves the direct alkylation of a PBI-based precursor amine and is performed in only three steps: (a) the condensation of PTCDA with putrescine, which yields the perylene bisamine **4**; (b) the alkylation of **4** to the corresponding tetraester **3** and (c) the quantitative removal of the *tert*-butyl protection group releasing the free acid **1a** with an overall yield of 11.6%.

The direct synthesis is primarily based on low cost chemicals and does not require the use of protected amine precursors such as amine **2**. Therefore, the outlined synthetic route provides the basis for a cost efficient large scale synthesis of these novel EDTA-PBI derivatives.

Nevertheless, the drawback of this approach is the alkylation of the derivative **4** due to its low solubility in the common suitable solvents for S_N2 reactions (*e.g.* CH_3CN), which is responsible for the relatively moderate overall yield.

With this knowledge in hand, the highly branched EDTA-PBIs **1b** and **1c** were synthesized solely according to a convergent approach (Schemes 2 and 3). The synthesis of the respective precursor amines **2**, **11** and **17** is reported in the ESI.† All the derivatives were fully characterized by ^{1}H- and ^{13}C-NMR and IR spectroscopy as well as by mass spectrometry and elemental analysis.

For the detailed investigation of the aggregation behavior of these novel compounds and for the direct comparison of their results with other commonly available chelating agents, the simplest derivative **1a** has been chosen and solution based optical measurements were carried out.

Compound **1a** exhibits a good solubility in basic ($NaOH_{(aq)}$, $c = 1 \times 10^{-3}$ M) as well as acidic ($HCl_{(aq)}$, $c = 1 \times 10^{-3}$ M) aqueous media. Among the common organic solvents, **1a** shows very good solubility only in dimethyl sulfoxide (DMSO). The solubility in organic solvents (such as DMSO; *N*-methyl pyrrolidone, methanol; *N*,*N*-dimethyl formamide and diethyl ether) can be drastically increased by the addition of acids like TFA, formic acid or hydrochloric acid ($HCl_{(aq)}$).

In the latter case, though, the introduction of water leads to a strong aggregation of the EDTA-PBI derivative by intermolecular π–π stacking interactions. These induced aggregation phenomena were investigated by ^{1}H-NMR spectroscopy as well as absorption and emission spectroscopy (ESI†).

Two aqueous (diluted acid and basic medium) and two organic (DMSO and DMSO with addition of TFA) solvents have been chosen to study the aggregation behavior of the EDTA-PBI derivative **1a**. For each system the most relevant optical properties have been determined and are listed in Table 1.

Normally, PBIs without functional moieties attached to the aromatic core can exist as aggregated as well as monomeric species in solution, depending on the solvent used.

In the case of monomeric PBIs, the distinct absorption band relative to the electronic transition $S_0 \rightarrow S_1$ is generally found in the range 400–600 nm and is characterized by three well resolved vibronic peaks. The predominant two features, located at ≈530 nm (0,0) and ≈490 nm (0,1), respectively, exhibit a ratio greater than 1.6.[34] Upon aggregation, pronounced modifications appear in the spectra. The intensity of the (0,0) peak is reduced, while that of the (0,1) peak increases accompanied by a pronounced reduction of the absorption coefficient.[17] The ratio between the (0,0) and (0,1) peaks reaches a value of ≈0.7 or lower in the case of strong aggregation.[29,35] As a result, the colour of the solution changes from orange to red.

As depicted in Fig. 3, **1a** is significantly aggregated, at room temperature, both under diluted basic ($NaOH_{(aq)}$, $c = 1 \times 10^{-3}$ M) and acid ($HCl_{(aq)}$, $c = 1 \times 10^{-3}$ M) aqueous conditions, due to the strong π–π stacking interactions of the perylene aromatic cores.

The behavior of **1a** can be explained as follows. Under basic aqueous conditions, pH ≈ 11, the EDTA-PBI is completely deprotonated (EDTA is completely deprotonated at pH > 10.6). Therefore, the aggregation proceeds most certainly *via* the formation of PBI stacked systems where each molecule is rotated with respect to its nearest neighbors. In such a way, the electrostatic repulsion of the residual charges situated at the periphery of each molecule would be minimized.[36]

In acid aqueous solution the aggregation is even more pronounced. As a matter of fact, at the pH under investigation (pH ≈ 3) it is impossible to have a complete protonation of **1a** due to the fact that the isoelectric point of **1a** is located at a value of pI = 2 or below.[37] We expect thus that **1a** exists in an equilibrium between several partly protonated species (H_xEDTA^{y+}, where $x < 4$ and $y < 2$) in solution. Therefore, no sufficient electrostatic repulsion is believed to hinder the aggregation by π–π stacking successfully. Moreover, the absorption spectrum of **1a** in diluted $HCl_{(aq)}$ shows a great broadening of the (0,1) peak in comparison with solutions of **1a** in diluted $NaOH_{(aq)}$ at the same concentration of the surfactant.

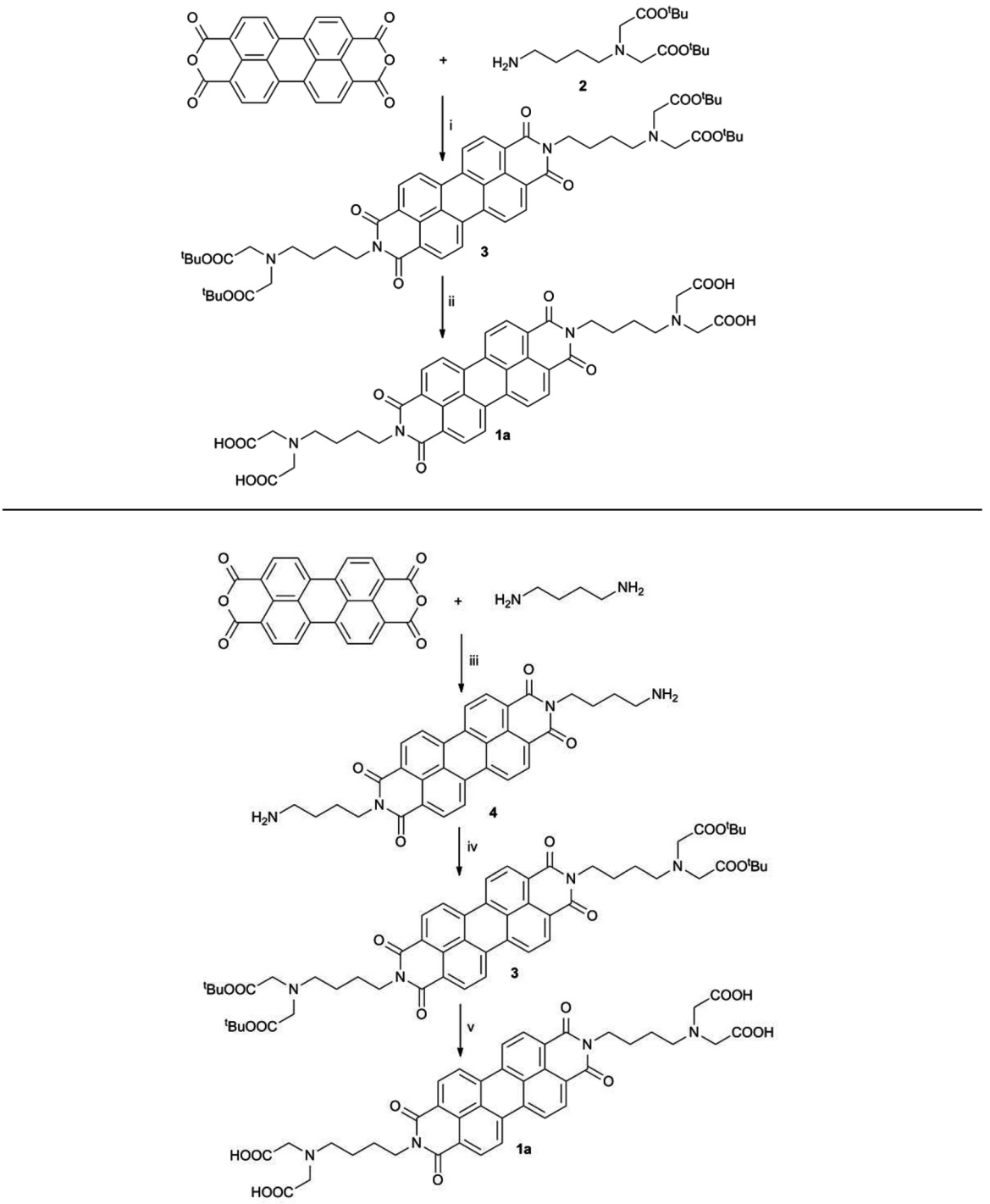

Scheme 1 Convergent (top) and direct (bottom) synthesis of EDTA-PBI **1a**. (i) Imidazole, $Zn(OAc)_2$, 110 °C, 4 h, yield: 64%; (ii) TFA–CH_2Cl_2 (2 : 1), rt, 5 days, yield: 84%; (iii) toluene, reflux, 4 h, yield: 89%; (iv) acetonitrile, DIPEA, *tert*-butyl bromoacetate, 60 °C, 24 h, yield: 13%; (v) formic acid, RT, 2 days, yield: 100%.

The enlargement of the (0,1) peak accounts generally for an extended aggregation in solution[17] and this confirms consequently that in diluted $HCl_{(aq)}$ the aggregation takes place more easily. In addition, further aggregation might derive from intermolecular hydrogen bonds between the protonated carboxylic moieties.

Furthermore, H-aggregates[38] are formed in aqueous solution both in diluted $NaOH_{(aq)}$ and $HCl_{(aq)}$. In both cases, the presence of PBI-dimers[39] is excluded.

In order to gain more insight into these aggregation phenomena, we decided to perform additional zeta potential measurements. The results are given in Table 2.

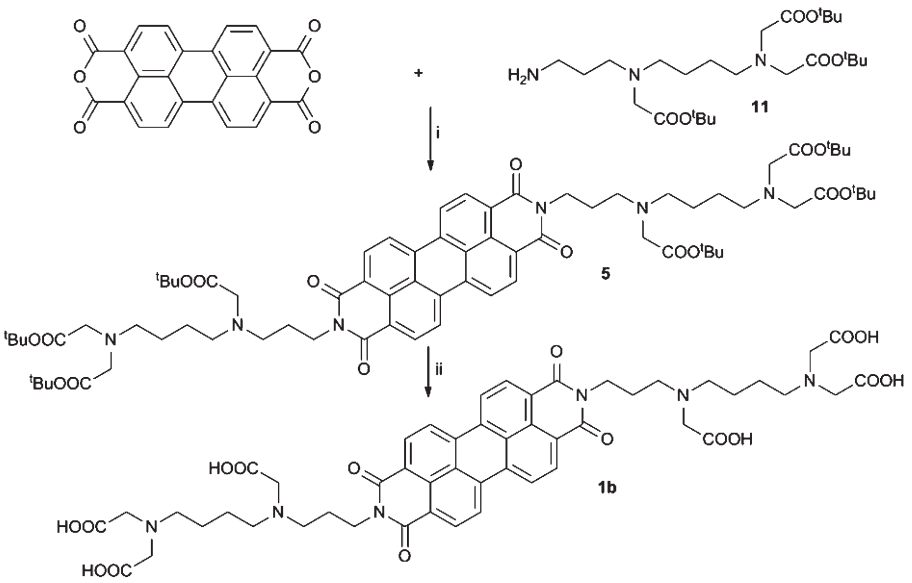

Scheme 2 Convergent synthesis of EDTA-PBI **1b**. (i) Imidazole, $Zn(OAc)_2$, 110 °C, 4 h, yield: 53%; (ii) TFA–CH_2Cl_2 (2 : 1), RT, 5 days, yield: 82%.

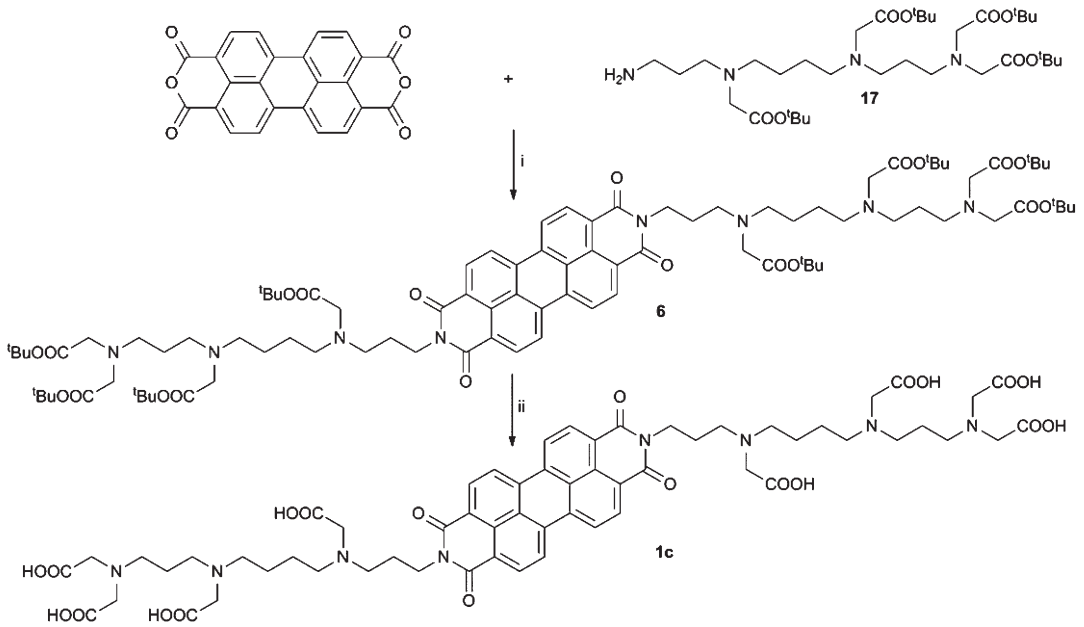

Scheme 3 Convergent synthesis of EDTA-PBI **1c**. (i) Imidazole, $Zn(OAc)_2$, 110 °C, 4 h, yield: 56%; (ii) TFA–CH_2Cl_2 (2 : 1), RT, 5 days, yield 74%.

Table 1 Optical properties of **1a** in aqueous and organic solvents

Property	$NaOH_{(aq)}$	$HCl_{(aq)}$	DMSO	H^+-DMSO[d]
$\log \varepsilon_{max}$ (M^{-1} cm^{-1})	4.38[b]	4.25[b]	4.53[c]	4.76[c]
$\lambda_{abs,\ max}$ (nm)	543, 500	549, 481	528, 494, 460	528, 494, 460
$\lambda_{fluo,\ max}$ (nm)	587, 546	587, 546	580, 543	580, 543
Φ (%)[a]	2.3 ± 0.2	0.27 ± 0.05	9.1 ± 1.1	63.9 ± 10.6

[a] The fluorescence quantum yield (Φ) is calculated taking fluorescein as the reference in NaOH 0.1 M.[33] [b] ε Calculated at 500 nm. [c] ε Calculated at 494 nm. [d] DMSO with addition of TFA, 3×10^{-4} M.

Zeta potential (ζ) measurements are used in order to predict the stability of dispersions. According to Greenwood *et al.*[40] a zeta potential value higher than ±30 mV indicates that a colloidal suspension is rather stable; moderate instability is characterized by a ζ value between ±10 mV and ±30 mV while extensive coagulation/flocculation occurs for a ζ value around 0 mV.

From the results given in Table 2, it is possible to conclude that **1a** is more stable in diluted $NaOH_{(aq)}$ than in diluted $HCl_{(aq)}$. However, in both cases the suspensions are rather unstable (ζ < 15 mV).

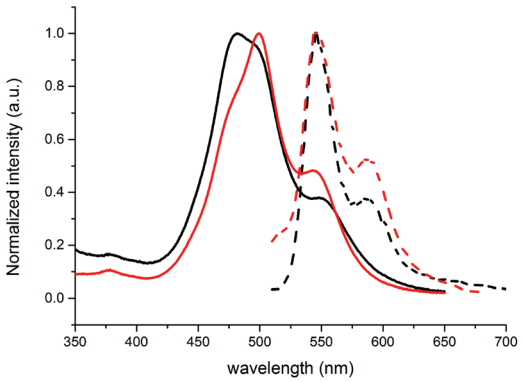

Fig. 3 Absorption and fluorescence profiles of **1a** in $NaOH_{(aq)}$ (red curve) and in $HCl_{(aq)}$ (black curve), $c = 5 \times 10^{-6}$ M.

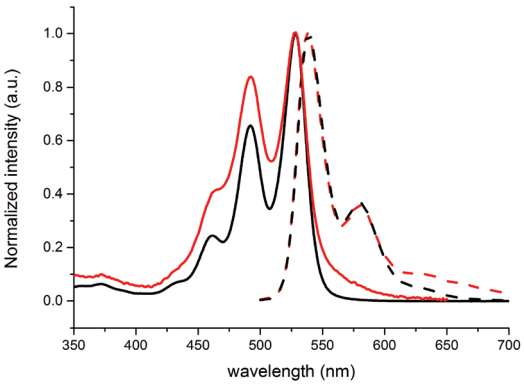

Fig. 4 Absorption and fluorescence profiles of **1a** in DMSO (red curve) and in acid–DMSO (black curve), $c = 5 \times 10^{-6}$ M.

Table 2 Zeta potential measurements of **1a** under aqueous conditions ($c = 1 \times 10^{-6}$ M)

Property	$NaOH_{(aq)}$, $c = 1 \times 10^{-3}$ M	$HCl_{(aq)}$, $c = 1 \times 10^{-3}$ M
Zeta potential (mV)	−13.3 ± 2.6	0.7 ± 0.7

The values of the UV and zeta potential measurements also corroborate with the fluorescence quantum yield data. Emission spectroscopy provides further insights into the equilibrium between monomeric and aggregated species. The dominant fluorescence can always be traced back to the monomeric species. In this case the emission profile is also the mirror image of the absorption spectrum. As aggregation takes place (Fig. 3) the absorption spectrum changes and therefore the emission does not appear any longer as the mirror image of the absorption spectrum.

As evidenced from Table 1, the fluorescence quantum yield (Φ) is approximately ten times lower for **1a** in diluted $HCl_{(aq)}$ than for **1a** in diluted $NaOH_{(aq)}$. Such drastically decreased Φ values in diluted $HCl_{(aq)}$ solutions might, however, appear counterintuitive. As a matter of fact, the tertiary amine functionalities, situated at both termini of the PBI acceptor aromatic core, determine a pronounced fluorescence quenching as a result of intra-molecular photo-induced electron transfer (PET).

Similar PBI dyes, which also bear bisamine functionalities linked to the perylene bisimide aromatic core, are generally characterized by an increase of the fluorescence either upon acid addition[19] or by chemical derivatization[41] and also in the presence of metal cations.[42] However, in diluted $HCl_{(aq)}$ it is observed that the aggregation process prevails over the amine protonation. The aggregation by π–π stacking contributes therefore to an overall fluorescence quenching even if the PET process might be partly suppressed.

When the aggregation in solution is prevented it is possible to examine the PET process in detail and to understand how it influences the fluorescence of PBI **1a**. For this study, we decided to investigate a solution of **1a** in DMSO, in the presence or absence of an acid. TFA was chosen due to the fact that the addition of diluted $HCl_{(aq)}$ would add water to the system, which leads to a more pronounced aggregation of **1a**.

First of all, in pure DMSO the behavior of **1a** is quite different (Fig. 4) from that in aqueous solutions at room temperature. As a matter of fact, the (0,0) peak is higher in intensity with respect to the (0,1) peak and their relative ratio is about 1.2. This value is lower than the threshold for completely monomeric PBIs, (0,0)/(0,1) ratio ≈1.6, and therefore we conclude that **1a** is present as a mixture of the monomeric and aggregated species in solution.

Due to the residual aggregation and because of the PET process, the fluorescence quantum yield of **1a** in DMSO remains pretty low (Φ < 10%) but five times higher with respect to the value measured in $NaOH_{(aq)}$ solutions, where the EDTA-PBI is strongly aggregated. Upon addition of a small amount of TFA to a DMSO solution of **1a** the fluorescence increases (Fig. 4) as a result of the protonation of the two tertiary amines, which lowers the energy of their nonbonding orbital below that of the HOMO of the PBI, allowing to switch on the fluorescence of the chromophore.[43] Under such conditions the fluorescence quantum yield increases drastically (Table 1). Concomitantly, due to protonation of the tertiary amines, the aggregation *via* π–π stacking is lowered and the solubility of **1a** is increased.

The possibility of switching on/off the fluorescence is remarkable and offers access to a broad range of applications for **1a** and analogue PBIs.[44–47] Moreover, as reported in the literature[48,49] it might be possible to correlate the fluorescence intensity with the pH and therefore obtain information about the acid/base equilibrium in solution. In our case, though, after the strong aggregation of **1a** took place, titration with either $NaOH_{(aq)}$ or $HCl_{(aq)}$ led to very little modifications of the fluorescence intensity and therefore hindered reliable determination of the six pK_as values of **1a**. However, due to the presence of a ligand periphery attached to a PBI reporter unit, derivative **1a** provides the possibility to investigate the coordination of metal ions in solution by means of spectroscopic measurements.

Both naphthalene[50,51] and perylene[52–58] based chelating agents have been reported, but to the best of our knowledge

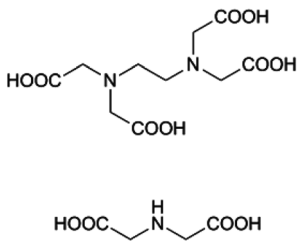

Fig. 5 Structures of EDTA (top) and IDA (bottom).

none of them with an elongated EDTA-like structure containing an integral PBI unit as an optical receptor unit.

As a matter of fact, the tailor-made periphery of **1a** was designed to efficiently chelate metal cations. The lock-and-key interaction of the metal cations with the tertiary amine functionalities at both sides of the EDTA-PBI will result in energy/electron transfer, which will be transmitted to the central PBI core *via* the PET process. By monitoring changes in the fluorescence of **1a** it can be defined as a set of parameters in order to determine the influence of different metals on the EDTA-PBI chromophore.

Of course, the aggregation by π–π stacking of **1a** in water and organic solvents will strongly influence the complexation of metal cations in solution. Such hydrophobic interactions could be responsible for the formation of a specific environment in solution which allows easier coordination of certain metal cations and not those expected for similar chelating agents, such as EDTA or iminodiacetic acid, IDA (Fig. 5).

The structure of **1a** resembles that of EDTA with the insertion of an integral PBI core between the two chelating moieties. Upon insertion, the separation between the two tertiary amine substituents is enhanced and an intramolecular EDTA-like coordination geometry (hexadentate ligand) is lost. However, an octahedral chelating geometry may be involved upon intermolecular interactions in solution, *e.g.* due to aggregation of the PBI molecules. Nevertheless, if in the aggregates the peripheral groups remain remote enough, the coordination geometry of **1a** should resemble more that of IDA (tridentate ligand).

Due to this complexity, we assume that the coordination geometry of **1a** in solution not only would be that of IDA or EDTA, but also would be more reasonably a mixture of both. The complexation of metal cations was investigated both in aqueous and organic media. Working in water based systems, on the one hand, is generally preferred for biological applications although in our case this means a stronger aggregation of the PBI aromatic moieties. In organic solvents, on the other hand, the π–π stacking is generally hindered but only niche applications can be addressed. Moreover, in non-aqueous systems it is more difficult to account for acid/base equilibria which may affect the complexation.

In order to gain the most comprehensive view of the affinity of **1a** for metal cations in aqueous solutions at room temperature, thirty common salts have been employed (ESI†). The first study was accomplished in distilled water, where **1a** is soluble only at concentrations below 10^{-5} M. As mentioned before, under aqueous conditions aggregation takes place easily. This has the following drawbacks. Above all, the fluorescence of **1a** is greatly quenched and therefore it is more difficult to discern the origin of the PET process. Moreover, the introduction of ion species in a solution where **1a** is already aggregated might also favor the formation of extended aggregates, which could be defined as supra-molecular polymers in solution.[59–67]

In a typical experiment, to a solution of **1a** in distilled water ($c = 5 \times 10^{-6}$ M), 10 equivalents of the chosen metal cations were added at room temperature. The solution was agitated mechanically for five minutes by means of a platform shaker and then the fluorescence spectrum was recorded and compared with a reference solution of **1a** in distilled water. The integrated fluorescence intensity in the presence (F) and absence (F_0) of the metal cation was determined subsequently and the results were compared in terms of their ratio (F/F_0). A value of F/F_0 higher than 1 indicates an enhancement of the fluorescence of the PBI (EF effect), while a value lower than 1 indicates a fluorescence quenching (QF effect).

The influence of the metal counter-ions has also been tested by addition of 10 equivalents of different sodium salts to a standard solution of **1a** in distilled water. The results show that different anions contribute on average to the same EF/QF in the presence of the same metal cations and therefore a counter-ion effect is generally excluded. The results of the complexation experiments for **1a** in an aqueous environment have been divided according to the charge of the respective cations (see ESI†). First of all, it can be noted that the addition of alkaline metal cations leads to an enhancement of the fluorescence of **1a** in water solutions only in the presence of K^+ and Cs^+, while this does not happen for Li^+ and Na^+. Alkaline earth metal ions have a negligible effect or induce a little decrease in the fluorescence intensity of **1a**.

These preliminary results suggest that most of the alkaline and alkaline earth cations are too small to interact efficiently with the chelating part of the EDTA-PBI. This might be explained considering the ionic radius of alkaline and alkaline earth metal cations. Actually K^+ and Cs^+ possess the highest values. Therefore, it might be argued that in a particular environment created by **1a** micelles in water solution only big cations can efficiently bind the nitrogen atom of the ligand side groups and slightly affect the PET process.

The addition of transition metals and lanthanides promotes, instead, a drastic fluorescence quenching ($F/F_0 < 0.16$), with the exception of Au^{3+} ($F/F_0 \approx 0.3$) and Ag^+ ($F/F_0 \approx 0.7$). In particular the most pronounced QF values were obtained for addition of copper ions (both Cu^+ and Cu^{2+}, QF = 0.0066) and trivalent cations (M^{3+} QF ≈ 0.01). Such a drastic fluorescence quenching is to be attributed to electron/energy transfer between the *d* electrons of the transition metals and the EDTA-PBI accepting molecules. As a matter of fact, the presence of transition metals or lanthanide cations leads to localized redox reactions (electron transfer) between the metal centers and the PBI moieties which result in the dramatic

quenching of the fluorescence of **1a**. Additionally, the metal cations might bridge vicinal PBI-micelles causing the formation of extended aggregates. This highly impressive fluorescence quenching is observed mainly for bivalent metal cations with the exception of Pb^{2+}, whose QF is not as pronounced ($F/F_0 \approx 0.4$) and also for Cu^{+}. Actually, Pb^{2+} is not a transition metal and a lower influence on the emission of the EDTA-PBI should be expected. Moreover, it is important to underline that a remarkable quenching of the fluorescence of **1a** can also be observed in the presence of metals with a d^{10} electronic configuration which cannot profit from ligand field effects, such as Zn^{2+}, Cd^{2+} and Hg^{2+}. Such metals do have a completely filled *d* level and cannot take part in any direct electron transfer process. However, it has been reported that depending on the geometry of the complex in solution other types of electron transfer processes may contribute to the quenching of the fluorescence of the chromophore.[68] In addition, De Santis *et al.*[69] showed that Zn^{2+} has a specific affinity towards carboxylic acid groups which may lead to a strong fluorescence quenching of the chromophore.

The addition of trivalent metal cations contributes, as well, to global quenching of the fluorescence of **1a**. In particular, the QF values are comparable to those recorded for copper cations ($F/F_0 \ll 0.1$). Nevertheless, the quenching of fluorescence is now accompanied by a strong modification of the emission spectrum of the EDTA-PBI molecule. As a matter of fact, the presence of trivalent metal cations induced the formation of a new broad band in the emission spectrum of **1a** (Fig. 6), which may account for the formation of emitting aggregated species (excimers) in solution.[70–75]

Furthermore, after a decantation of 2–3 days, the solutions of **1a** titrated with 10 equivalents of M^{3+} become transparent and a solid precipitate was formed. The new broadened feature present in the emission spectrum of **1a**, which is not present in the normal emission spectrum of **1a** under aqueous conditions, is located between 660 and 680 nm and the λ_{max} of the peak shifts depending on the metal cation added (Sm^{3+} $\lambda_{max} \approx$ 660 nm, QF ≈ 0.05; In^{3+}, Gd^{3+} and La^{3+} $\lambda_{max} \approx$ 670 nm, QF ≈ 0.01; Fe^{3+} and Sc^{3+} $\lambda_{max} \approx$ 675 nm, QF < 0.01; Ce^{3+} $\lambda_{max} \approx$ 680 nm, QF ≈ 0.01). The formation of this new band in the emission spectrum of PBIs has been extensively discussed in the literature. According to Wang *et al.*[35,76–78] who examined the self-organization of a PEG functionalized PBI in chloroform solution, such a red shifted band in the emission spectrum of PBIs may be attributed to the fluorescence properties of molecular assemblies of increased size. The same conclusions have also been outlined by Neuteboom and coworkers[79] when studying the optical features of polytetrahydrofuran substituted PBI polymers in ODCB. Arnaud *et al.*,[71] Würthner *et al.*,[70,80,81] Datar *et al.*,[82] and Yagai *et al.*[75] reported as well the formation of this red-shifted band due to self-assembled/polymeric PBI in solutions.

To probe the stability of these metal-induced aggregated emitting species in solution, temperature dependent fluorescence measurements have been performed. As depicted in Fig. 7, an increase in temperature (from 25 °C to 75 °C) leads normally to an increase of the F/F_0 value and this correlates with a lower aggregation in solution. This observation corroborated with a decrease in intensity and eventually with the disappearance of the band situated between 660 and 680 nm in the fluorescence spectrum. The only exception to this pattern is found for In^{3+}.

Considering that for the other metal cations such a band vanishes around 45 °C, we assume a higher stability for **1a**-In^{3+} complexes and therefore presumably a higher binding constant. For this cation in fact, the F/F_0 ratio remains practically constant even at higher temperatures and the band due to PBI excimers persists till 65 °C.

Additionally, with the help of Van't Hoff plots (see ESI†), it is possible to evaluate the thermodynamic parameters associated with the denaturation process. As a matter of fact, as the temperature increases the supramolecular structures based on PBI agglomerates coordinated to metal ions tend to disaggregate in solution. In detail, the F/F_0 ratio can be considered proportional to the equilibrium constant of the process (K_{eq}) and a plot of $\ln(F/F_0)$ *vs.* T^{-1} can thus provide information about the standard enthalpy ($\Delta H°$) and entropy ($\Delta S°$) of the denaturation process for each ion. As shown in the ESI,† the plots $\ln(F/F_0)$ *vs.* T^{-1} are linear only at temperatures above 45 °C.

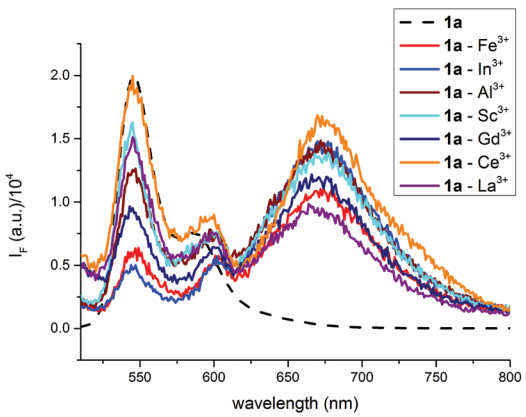

Fig. 6 Fluorescence spectra of **1a** in water after addition of 10 eq. of M^{3+} (Sm^{3+} is not shown for clarity, due to its higher QF value).

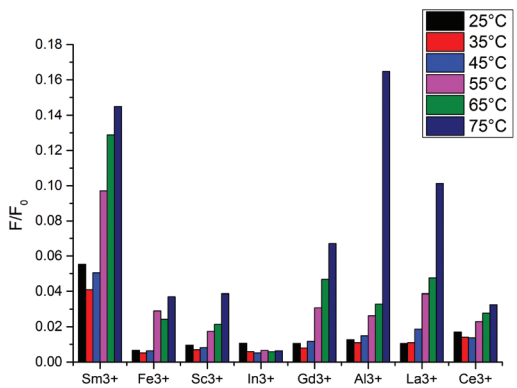

Fig. 7 Temperature dependent fluorescence spectra of **1a** in water after addition of 10 eq. of M^{3+}.

Therefore, we assumed that both parameters are temperature dependent and decided to extrapolate their values only in the temperature interval 45 °C ≤ T ≤ 75 °C. With the exception of Ce^{3+} and Sm^{3+} $\Delta H°$ can be determined to be 54.1 ± 1.5 kJ mol^{-1} and $\Delta S°$ to be 15.9 ± 2.7 J mol^{-1}. For the former ions, $\Delta H°$ can be calculated as 16.2 ± 1.3 kJ mol^{-1} and 31.9 ± 2.1 kJ mol^{-1} and $\Delta S°$ as 2.2 ± 0.3 J mol^{-1} and 9.2 ± 0.4 J mol^{-1}, respectively. In the case of In^{3+} no calculation was carried out due to the fact that the denaturation process appears not to take place in the temperature range studied. The positive enthalpy and entropy values indicate that the denaturation of the metal-induced aggregates of **1a** in solution is an endothermic process and therefore favored at high temperatures.

So far, we have described the complexation of **1a** under aqueous conditions, where **1a** is aggregated and the introduction of trivalent metal ions most likely triggers the formation of PBI emitting aggregates in solution.

In order to gain more insights into the interaction of the EDTA-PBI with metal cations in solution, it has been decided to add the metal ions to **1a** in the water–DMSO mixture. As mentioned above, **1a** is predominantly present as a monomer in DMSO and these conditions should provide a better visualization of the true interaction of a single PBI molecule with the metal cation in solution. DMSO–water systems have been very well studied in the literature.[83–86] Due to the complex interactions of water and DMSO molecules, which lead for example to a pronounced melting point depression for a DMSO molar fraction (x_{DMSO}) of about 0.33[87] it would be difficult to attempt a detailed description of the effect of metal ions on the PET of **1a** over the entire molar fraction range. Therefore, we preferred to focus our attention on the region of 0.8 ≤ x_{DMSO} ≤ 1 (the so-called DMSO-rich region). Moreover, in order to ensure sufficient solubility of the metal salts and to avoid as much as possible the hydrophobic effect, it was decided to work with mixtures where x_{DMSO} = 0.9.

Five salts of transition metals were chosen to be investigated. Namely, three divalent (Ni^{2+}, Co^{2+} and Cu^{2+}) and two trivalent (Al^{3+} and Fe^{3+}) metal ions have been tested. These five metal cations were selected among those who should form the most stable complexes with IDA and EDTA moieties. First of all, absorption measurements have been performed to investigate the influence of these metal cations on the spectroscopic properties of **1a**. As the EDTA-PBI is mostly present as a monomer in solution, absorption spectroscopy can provide precious information about the metal complexation (Fig. 8).

The addition of bivalent and trivalent metal cations to the EDTA-PBI solution results generally in a global decrease of the intensity of the absorption bands and in a lower value of the $I_{529/493}$ ratio. As described before, a decrease in the latter parameter accounts for the formation of aggregates in solution. In particular, these effects are strictly dependent on the metal ion and were recorded to be maximal for Co^{2+} and Al^{3+}. Further proof of the interaction between **1a** and the metal cations in DMSO-rich solutions is given by fluorescence spectroscopy measurements. In DMSO-rich solution **1a** is still mainly present as a monomer in solution.

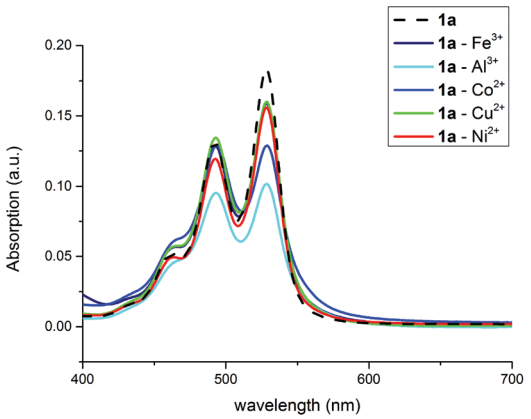

Fig. 8 Absorption spectra of **1a** in the DMSO–water mixture (9 : 1) after addition of 10 eq. of M^{x+}.

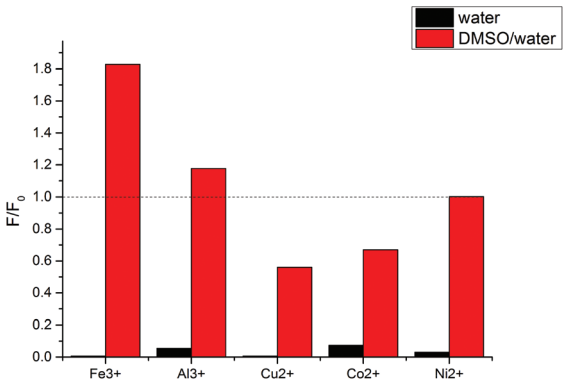

Fig. 9 Comparison of the F/F_0 ratios for complexes of **1a** with M^{2+} and M^{3+} in a DMSO–water (9 : 1) mixture.

Upon addition of divalent metal cations, quenching of the PBI fluorescence is observed, most likely due to the electron transfer processes from the metal center to the aromatic core. The affinity for trivalent metal cations remains high as well. In DMSO-rich solutions, however, the addition of trivalent cations is now correlated with an enhanced fluorescence of **1a** (Fig. 9). The presence of predominant monomeric species in solution allows a successful interaction of the EDTA-PBI with the metal cations which lead to a drastic quenching of the PET process (Al^{3+} EF ≈ 1.18; Fe^{3+} EF ≈ 1.83).

Conclusion

In this contribution the first representatives of a new class of perylene bisimide-based surfactants are reported. In particular, the synthesis, optical characterization and metal complexation ability of the PBI derivative **1a** were investigated in detail. Two reasonable synthetic pathways, leading to the target structure **1a**, have been elaborated and discussed. The full optical characterization (UV/Vis and emission spectroscopy) has been reported both under aqueous and organic conditions. In the former solvent a detailed study of the aggregation behavior has

been presented on the basis of absorption as well as fluorescence data and zeta potential measurements, both under basic and acidic conditions.

Moreover, the influence of the intra-molecular PET process on the spectroscopic properties of dye **1a** in DMSO solution has been described. It has also been shown that upon addition of an acid the PET process can be suppressed and the peculiarity of the phenomenon has been discussed with regard to feasible applications. For example, it could be imagined to fully exploit this pH-driven fluorescence sensitivity to develop EDTA-PBI water soluble sensors. Furthermore, a detailed investigation of the complexation of metal cations both in water and DMSO–water mixtures has been offered. This study revealed the importance of the aggregation state of the EDTA-PBI in the complexation properties of **1a**. Under aqueous conditions, where bulky aggregates prevail, only big alkaline metal cations lead to the suppression of the PET process. Bi- and trivalent cations were responsible for a pronounced fluorescence quenching (QF). Additionally, the complexation of trivalent metal ions is characterized by the formation of emitting aggregate species (excimers), which modify profoundly the emission spectrum of the EDTA-PBI itself. The origin and stability of these species were discussed by means of temperature dependent fluorescence spectroscopy and In^{3+} has been observed to form the strongest complexes, among the metal cations tested. A strong affinity of **1a** for di- and trivalent metal ions has been demonstrated in DMSO-rich solutions as well. The former metal cations are involved in energy/electron transfer also with predominantly monomeric PBIs. The addition of the latter results, instead, in a strong fluorescence enhancement (EF).

The intriguing structure of derivatives **1a–c** which combines namely an electron deficient central aromatic structure (PBI core), a polycarboxylic backbone and a chelating periphery renders them suitable for many applications. Among the most appealing ideas, it would be interesting to exploit the potential of **1a** for the aqueous exfoliation of carbon allotropes or other 2D-layered inorganic materials, such as molybdenum disulphide (MoS_2) or tungsten disulphide (WS_2). In the latter case, in fact, it is known that specific ions (like Ni^{2+} or Al^{3+}) are used to create inclusion during the exfoliation process and help to hinder the re-stacking of the dispersed material.[88]

Finally, the results of the complexation study, collected both under aqueous and organic conditions, underline the striking affinity of **1a** for heavy trivalent metal ions. The identification of such a successful interaction of transition metals and lanthanide cations with EDTA-PBIs opens up the way to challenging application in water decontamination, *e.g.* the detection of hard metals which is of extreme environmental importance.

Experimental section

Materials and methods

Reagents and solvents were purchased from Acros Organics, Sigma Aldrich and used without further purification. Moisture sensitive reactions were performed under a N_2 atmosphere. CH_2Cl_2 was distilled over CaH_2, THF over Na/benzophenone and DMF dried over 4 Å molecular sieves. Chromatographic purifications were performed with silica gel from Merck (Kieselgel 60, 40–60 μm, 230–400 mesh ASTM) in standard glass columns. TLC was performed on aluminium sheets coated with silica gel from Merck (F254). ^1H and ^{13}C NMR spectra were recorded with a Brucker AV500 (500 MHz for ^1H and 125 MHz for ^{13}C) spectrometer, a Jeol JNM EX 400 (400 MHz for ^1H and 100 MHz for ^{13}C) and a Jeol Brucker Avance 300 (300 MHz for ^1H and 75 MHz for ^{13}C) spectrometer. Chemical shifts are reported in ppm at room temperature (RT) using $CDCl_3$ as the solvent and the internal standard, unless otherwise indicated. Abbreviations used for splitting patterns are s = singlet, d = doublet, t = triplet, m = multiplet, and dd = double doublet. IR spectra were recorded with a FT-IR Nicolet 5700, a Brucker Tensor 27 (ATR) and an ASI React IRTM 1000 spectrometer. For UV/Vis spectra a Perkin Elmer Lambda 1050 was used. Fluorescence was measured with a Horiba Scientific Fluorolog-3 spectrometer with a PMT detector. MALDI-TOF mass spectrometry was carried out on a Shimadzu AXIMA Confidence, N_2 UV laser (337 nm), 50 Hz (reflectron). The matrices used were 2′,4′,6′-trihydroxyacetophenone monohydrate (THAP), 2,5-dihydoxybenzoic acid (DHB), 3,5-dimethoxy-4-hydroxycinnamic acid (SIN) and 2-[(2*E*)-3-(4-*tert*-butylphenyl)-2-methylprop-2-enylidene] malonitrile (DCTB). ESI mass spectrometry was performed with an Agilent Technologies 1100 Series LC/MSD Trap-SL spectrometer equipped with an ESI source, a hexapole filter and an ionic trap and Brucker maXis 4G. Zeta-potential measurements were carried out on a Malvern Zetasizer Nano system with irradiation from a 633 nm He–Ne laser. The solution of **1a** with the metal cations were prepared by mechanically stirring the solutions with a Heidolph Unimax 1010 platform shaker. For elemental analyses, a CE instrument EA 1110 CHNS was used.

In the following the syntheses of the different PBI derivatives are presented. The synthesis of the amine precursors **2**, **11** and **17** is presented in the ESI.† Compound **4** was prepared according to a slightly modified procedure adapted from Xue *et al.*[89] For the putrescine based derivative **1a**, the direct synthesis is defined as *route i*, while the convergent synthesis is defined as *route ii*.

***N*-Bis-(4-aminobutane)-3,4,9,10-PBI (4).** [route i]: A mixture of PTCDA (10 g, 2.6×10^{-2} mol) and 1,4-diaminobutane (4 eq.) in toluene (250 mL) was stirred at reflux (110 °C) for 4 hours. After cooling down to room temperature, the mixture was filtered under vacuum and washed with toluene. The crude solid was then re-suspended in KOH 5 M (200 mL) and stirred for 15 hours at ambient temperature. Subsequently, the suspension was filtered and **4** was collected as a red-brownish solid, which was dried under vacuum (16.4 g, yield = 89%).

^1H NMR (500 MHz, DMSO-d_6 + TFA): δ = 1.65–1.76 (8H, 2 m, $4CH_2$), 2.89 (4H, m, $2CH_2CH_2NH_3^+$), 4.07 (4H, t, $2NCH_2CH_2$), 7.74 (6H, t, $2CH_2NH_3^+$), 8.30 (4H, d, ArH), 8.55 (4H, d, 4ArH) ppm.

ESI-MS: m/z 533.3 $(M + H)^+$, 267.2 $(M + 2H)^{2+}$.

IR (KBr disc): ν = 3350, 3300 (primary amine, $-NH_2$ stretching); 2927, 2849 (stretching $-CH_2$); 1690, 1653 (stretching C=O bisimide) cm^{-1}.

***N*-Bis-(*tert*-butyl-(2,2′-aminobutylazanediyl)-diacetate)-3,4,9,10 PBI (3).** [route i]: A mixture of **4** (280 mg, 5.3×10^{-4} mol), acetonitrile (15 mL), DIPEA (10 eq.) and *tert*-butyl bromoacetate (8 eq.) was stirred at 60 °C for 24 hours. Once cooled down to room temperature, it was vacuum filtered and the crude solid was washed with acetonitrile and water. Subsequently the solid residue was dissolved in chloroform (5 mL) and hexane was added (100 mL). The mixture was stirred for 10 minutes at room temperature and then allowed to stand for one night. The precipitate was filtered and dried under vacuum. **3** is isolated as a brown solid (70 mg, yield = 13%).

[route ii]: Precursor amine **2** (404 mg, 1.3×10^{-3} mol), PTCDA (250 mg, 6.4×10^{-4} mol), imidazole (868 mg) and zinc acetate (35 mg) were mixed and heated up to 110 °C for 4 h. Afterwards, dichloromethane was added to the solid residue and column chromatography in CH_2Cl_2–EtOH (98 : 2) was performed to isolate a red solid, **3** (404 mg, yield = 64%).

^{1}H NMR (300 MHz, $CDCl_3$, 25 °C): δ = 1.44 (s, 36H, 12 × CH_3), 1.63 (quintuplet, J = 7.0 Hz, 4H, 2 × CH_2), 1.79 (quintuplet, J = 7.5 Hz, 4H, 2 × CH_2), 2.77 (t, J = 7.6 Hz, 4H, 2 × CH_2), 3.44 (s, 8H, 4 × NCH_2), 4.21 (t, J = 7.4 Hz, 4H, 2 × CH_2), 8.33 (d, J = 8.0 Hz, 4H, ArH), 8.48 (d, J = 8.0 Hz, 4H, ArH) ppm.

^{13}C NMR (75 MHz, $CDCl_3$, 25 °C): δ = 25.536 (2 C, CH_2), 25.641 (2 C, CH_2), 28.049 (12 C, CH_3), 40.267 (2 C, CH_2), 53.864 (2 C, CH_2), 55.732 (4 C, CH_2), 80.732 (4 C, quat. C ^{t}Bu), 122.469 (4 C, Ar-CH), 122.850 (2 C, Ar-C), 125.388 (2 C, Ar-C), 128.552 (4 C, Ar-C), 130.625 (4 C, Ar-CH), 133.581 (4 C, Ar-C), 162.762 (4 C, CON), 170.773 (4 C, COO) ppm.

MALDI-TOF (THAP): m/z 989 $(M + H)^+$, 1011 $(M + Na)^+$.

IR (ATR): ν = 2976.44, 2932.02, 1731.53, 1692.97, 1654.17, 1594.27, 1340.47, 1251.21, 1215.23, 1142.65, 988.15, 809.48, 745.88 cm^{-1}.

EA for $C_{56}H_{68}N_4O_{12}$: calcd C 68.00, H 6.93, N 5.66; found C 67.66; H 6.90; N 5.65.

***N*-Bis-(*tert*-butyl-(2,2′-aminobutylazanediyl)-diacetic acid)-3,4,9,10-PBI (1a).** [route i]: A solution of **3** (520 mg, 5.3×10^{-4} mol) in formic acid (20 mL) was stirred at room temperature for 2 days. Acetonitrile (20 mL) was added and a solid precipitated. The solvent was evaporated *in vacuo*. The crude solid was washed two times with acetonitrile and once with diethyl ether. **1a** is isolated as a reddish solid (400 mg, quantitative yield).

[route ii]: A solution of **3** (250 mg, 2.5×10^{-4} mol) in TFA–CH_2Cl_2 (1 : 1) was stirred at room temperature for 5 days. After evaporation of the solvent, the product was precipitated by addition of diethylether. The solid was filtered and dried *in vacuo*. A red-brown solid was obtained (160 mg, yield = 84%).

^{1}H NMR (300 MHz, $CDCl_3$, 25 °C): δ = 1.99–2.06 (m, 8H, 4 × CH_2), 3.69 (t, J = 7.4 Hz, 4H, 2 × CH_2), 4.39 (t, J = 6.6 Hz, 4H, 2 × CH_2), 4.45 (s, 8H, 4 × NCH_2), 8.80–8.86 (m, 8H, perylene ArH) ppm.

^{13}C NMR (75 MHz, $CDCl_3$, 25 °C): δ = 22.080 (2 C, CH_2), 24.631 (2 C, CH_2), 40.479 (2 C, CH_2), 55.547 (2 C, CH_2), 58.388 (4 C, CH_2), 122.430 (2 C, Ar-C), 124.888 (4 C, Ar-CH), 126.837 (2 C, Ar-C), 129.781 (4 C, Ar-C), 133.566 (4 C, Ar-CH), 136.483 (4 C, Ar-C), 166.146 (4 C, CON), 169.575 (4 C, COO) ppm.

MALDI-TOF (DHB): m/z 649 $(MH - 2CH_2CO_2)^+$, 708 $(MH - CH_2CO_2)^+$, 765 $(M + H)^+$, 787 $(M + Na)^+$.

IR (ATR): ν = 3468.87, 3016.23, 2969.14, 2547.61, 1735.46, 1687.25, 1645.08, 1593.03, 1576.71, 1441.85, 1402.08, 1381.67, 1341.39, 1246.11, 1169.21, 1137.12, 1088.06, 809.08, 794.31, 744.42, 719.63 cm^{-1}.

EA for $C_{46}H_{39}F_9N_4O_{18}$ (765) × $3CF_3COOH$: calcd C 49.92, H 3.55, N 5.06; found C 49.37; H 4.10; N 4.96.

Tetra-*tert*-butyl 2,2′,2″,2‴((1,3,8,10-tetraoxoanthra[2,1,9-def:6,5,10-*d*′*e*′*f*′]di-isoquinoline-2,9(1*H*,3*H*,8*H*,10*H*)-diyl)bis-(propane-3,1diyl)-bis(((2-(*tert*-butoxy)-2-oxoethyl)azanediyl)bis-(butane-4,1-diyl))bis(azanetriyl))-tetraacetate (5). Precursor amine **11** (0.62 g, 1.3 mmol), PTCDA (0.25 g, 0.64 mmol), imidazole (0.87 g, 13.0 mmol) and zinc acetate (0.035 g, 0.2 mmol) were heated at 110 °C for 4 h. Afterwards, dichloromethane was added and the solid residue was purified by column chromatography (SiO_2, dichloromethane–ethanol, 95 : 5). **5** is isolated as a red solid (gummy) (1.9 g, yield = 53.3%).

^{1}H NMR (300 MHz, $CDCl_3$): δ = 1.43 (s, 18H, 6 × CH_3), 1.44 (bs, 36H, 12 × CH_3) 1.47–1.48 (m, 4H, 2 × CH_2), 1.74 (broad quintuplet, 4H, 2 × CH_2), 1.92 (quintuplet, J = 7.2 Hz, 4H, 2 × CH_2), 2.63 (t, J = 6.8 Hz, 4H, 2 × CH_2), 2.68 (t, J = 7.0 Hz, 4H, 2 × CH_2), 2.78 (t, J = 7.0 Hz, 4H, 2 × CH_2), 3.30 (s, 4H, 2 × NCH_2), 3.41 (s, 8H, 4 × NCH_2), 4.24 (t, J = 7.6 Hz, 4H, 2 × CH_2), 8.51 (d, J = 8.0 Hz, 4H, ArH), 8.61 (d, J = 8.0 Hz, 4H, ArH) ppm.

^{13}C NMR (75 MHz, $CDCl_3$): δ = 25.18 (2 C, CH_2), 25.66 (2 C, CH_2), 25.87 (2 C, CH_2), 28.04 (6 C, CH_3), 28.07 (12 C, CH_3), 38.91 (2 C, CH_2), 51.76 (2 C, CH_2), 53.73 (2 C, CH_2), 54.06 (2 C, CH_2), 55.14 (2 C, CH_2), 55.72 (4 C, CH_2), 80.56 (2 C, quat. C ^{t}Bu), 80.70 (4 C, quat. C ^{t}Bu), 122.71 (4 C, Ar-CH), 123.07 (2 C, Ar-C), 125.83 (2 C, Ar-C), 128.90 (4 C, Ar-C), 130.91 (4 C, Ar-CH), 133.99 (4 C, Ar-C), 162.99 (4 C, CON), 170.79 (4 C, COO), 170.95 (2 C, COO) ppm.

MS-ESI(+): m/z = 1332 $[M^+ + H]$.

IR (ATR): ν = 2975.77, 2933.03, 2865.49, 1729.00, 1694.37, 1655.12, 1594.05, 1440.45, 1402.63, 1365.62, 1345.19, 1247.93, 1216.78, 1145.75, 1069.42, 848.50, 809.39, 744.38 cm^{-1}.

EA for $C_{74}H_{102}N_6O_{16}$: calcd C 66.74, H 7.72, N 6.31; found C 66.30; H 7.80; N 6.35.

2,2′,2″,2‴-((1,3,8,10-Tetraoxoanthra[2,1,9-def:6,5,10-*d*′*e*′*f*′]-diisoquinoline-2,9(1*H*,3*H*,8*H*,10*H*)-diyl)bis(propane-3,1diyl)bis-(((carboxymethyl)azanediyl)-bis(butane-4,1-diyl))bis(azanetriyl))-tetraacetic acid (1b). **5** (0.5 g, 0.37 mmol) was dissolved in 18 mL of TFA. The reaction mixture was stirred for 3 days at room temperature. After evaporation of the solvent, the product was precipitated on addition of diethyl ether. After filtration, the product was dried under vacuum. **1b** is isolated as a dark red solid (0.30 g, yield = 81.9%).

^{1}H NMR (300 MHz, TFA–$CDCl_3$; (1 : 1)): δ = 1.85 (bq, 8H, 4 × CH_2), 2.25 (bq, J = 6.8 Hz, 4H, 2 × CH_2), 3.33–3.46 (m, 12H, 6 ×

CH_2), 4.02–4.30 (m, 12H of 6 × NCH_2 superimposed with 4H protons of 2 × CH_2), 8.61 (d, J = 7.6 Hz, 4H, perylene ArH), 8.67 (d, J = 8.4 Hz, 4H, perylene ArH) ppm.

MS-ESI(+): m/z = 996 [M^+ + 2H].

IR (ATR): ν = 3016.80, 2973.38, 2546.03, 1735.01, 1691.09, 1649.09, 1593.05, 1577.36, 1401.75, 1343.23, 1172.33, 1129.89, 809.29, 794.60, 719.90 cm^{-1}.

EA for $C_{50}H_{54}N_6O_{16}$ × $5CF_3COOH$: calcd C 46.04, H 3.80, N 5.37; found C 45.74; H 4.29; N 5.07.

Tetra-*tert*-butyl 2,2′,2″,2‴-(11,11′-((1,3,8,10-tetraoxoanthra-[2,1,9-def:6,5,10-*d′e′f′*]diisoquinoline-2,9(1*H*,3*H*,8*H*,10*H*)-diyl)-bis(propane-3,1-diyl-bis(2,2,15,15-tetramethyl-4,13-dioxo-3,14-dioxa-6,11-diazahexadecane-11,6-diyl-bis(propane-3,1-diyl)))bis-(azanetriyl))tetraacetate (6). Precursor amine **17** (0.25 g, 0.38 mmol), PTCDA (0.07 g, 0.17 mmol), imidazole (0.24 g, 3.46 mmol) and zinc acetate (0.01 g, 0.05 mmol) were heated at 110 °C for 4 h. Afterwards, dichloromethane was added to the solid residue and the residue was purified by column chromatography (SiO_2, dichloromethane–ethanol, 95 : 5). **6** is isolated as a dark red solid (0.22 g, yield = 74.3%).

^{1}H NMR (300 MHz, $CDCl_3$): δ = 1.41–1.42 (s, 72H, 24 × CH_3. This multiplet superimposes on the signals of 8H protons of 4 × CH_2), 1.61 (quintuplet, J = 6.9 Hz, 4H, 2 × CH_2), 1.91 (quintuplet, J = 7.0 Hz, 4H, 2 × CH_2), 2.57–2.60 (m, 12H, 6 × CH_2), 2.68 (t, J = 7.4 Hz, 4H, 2 × CH_2), 2.77 (t, J = 7.0 Hz, 4H, 2 × CH_2), 3.20 (s, 4H, 2 × NCH_2), 3.28 (s, 4H, 2 × NCH_2), 3.40 (s, 8H, 4 × NCH_2), 4.22 (t, J = 7.4 Hz, 4H, 2 × CH_2), 8.43 (d, J = 8.0 Hz, 4H, ArH), 8.55 (d, J = 8.0 Hz, 4H, ArH) ppm.

^{13}C NMR (75 MHz, $CDCl_3$): δ = 25.219 (2 C, CH_2), 25.372 (2 C, CH_2), 25.884 (2 C, CH_2), 26.056 (2 C, CH_2), 28.023 (12 C, CH_3), 28.040 (6 C, CH_3), 28.064 (6 C, CH_3), 38.906 (2 C, CH_2), 51.789 (2 C, CH_2), 51.885 (2 C, CH_2), 52.113 (2 C, CH_2), 53.805 (2 C, CH_2), 54.220 (2 C, CH_2), 55.191 (2 C, CH_2), 55.519 (2 C, CH_2), 55.704 (4 C, CH_2), 80.482 (4 C, quat. C ^{t}Bu), 80.523 (2 C, quat. C ^{t}Bu), 80.684 (2 C, quat. C ^{t}Bu), 122.776 (4 C, Ar-CH), 123.101 (2 C, Ar-C), 125.908 (2 C, Ar-C), 128.952 (4 C, Ar-C), 130.956 (4 C, Ar-CH), 134.072 (4 C, Ar-C), 163.032 (4 C, CON), 170.728 (4 C, COO), 170.923 (4 C, COO) ppm.

MS-ESI(+): m/z = 1675 [M^+ + 2H].

IR (ATR): ν = 2976.98, 2935.25, 1727.43, 1695.03, 1655.53, 1594.39, 1365.73, 1247.92, 1216.67, 1144.99, 848.11, 809.43, 744.48 cm^{-1}.

EA for $C_{92}H_{136}N_8O_{20}$: calcd C 66.00, H 8.19, N 6.69; found C 64.87; H 8.65; N 6.56.

2,2′,2″,2‴-((1,3,8,10-Tetraoxoanthra[2,1,9-def:6,5,10-*d′e′f′*]-diisoquinoline-2,9(1*H*,3*H*,8*H*,10*H*)-diyl)bis(propane-3,1diyl)-bis(((carboxymethyl)azanediyl)bis(butane-4,1-diyl))-bis(((carboxy-methyl)azanediyl)bis(propane-3,1diyl))bis-(azanetriyl))tetra-acetic acid (1c). (0.23 g, 0.14 mmol) was dissolved in 18 mL TFA. The reaction mixture was stirred for 6 days at RT. After evaporation of the solvent, the product was precipitated on addition of diethyl ether. After filtration, the product was dried under vacuum. **1c** is isolated as a dark red solid (9.4 mg, yield = 56.2%).

^{1}H NMR (300 MHz, TFA–$CDCl_3$; (1 : 1)): δ = 1.99 (broad quintuplet, 8H, 4 × CH_2), 2.41 (broad quintuplet, 4H, 2 × CH_2), 2.50 (broad quintuplet, 4H, 2 × CH_2), 3.49 (bt, 8H, 4 × CH_2), 3.57 (bt, 8H, 4 × CH_2), 3.68 (bt, 8H, 4 × CH_2), 4.21 (s, 4H, 2 × NCH_2), 4.39 (s, 12H, 6 × NCH_2), 8.78 (d, J = 6.0 Hz, 4H, ArH), 8.84 (d, J = 6.0 Hz, 4H, ArH) ppm.

MS-ESI(+): m/z = 1226 [M^+ + 2H].

IR (ATR): ν = 2976.98, 2935.25, 1727.43, 1695.03, 1655.53, 1594.39, 1365.73, 1247.92, 1216.67, 1144.99, 848.11, 809.43, 744.48 cm^{-1}.

EA for $C_{60}H_{72}N_8O_{20}$ × $5CF_3COOH$: calcd C 46.83, H 4.32, N 6.24; found C 45.66; H 4.38; N 6.12.

Acknowledgements

MM, FH and AH thank the Deutsche Forschungsgemeinschaft (DFG – SFB 953, Project A1 "Synthetic Carbon Allotropes") and the Interdisciplinary Center for Molecular Materials (ICMM) for the financial support. The research leading to these results has partially received funding from the European Union Seventh Framework Programme under grant agreement no. 604391 Graphene Flagship. PS is thankful to the Alexander von Humboldt foundation for granting the AvH research Fellowship.

Notes and references

1 F. Wurthner, *Chem. Commun.*, 2004, 1564.
2 T. Weil, T. Vosch, J. Hofkens, K. Peneva and K. Mullen, *Angew. Chem., Int. Ed.*, 2010, **49**, 9068.
3 C. Li and H. Wonneberger, *Adv. Mater.*, 2012, **24**, 613.
4 M. Ramesh, H. C. Lin and C. W. Chu, *Biosens. Bioelectron.*, 2013, **42**, 76.
5 Y. Li, T. Liu, H. Liu, M. Z. Tian and Y. Li, *Acc. Chem. Res.*, 2014, **47**, 1186.
6 A. Ringk, X. R. Li, F. Gholamrezaie, E. C. P. Smits, A. Neuhold, A. Moser, C. Van der Marel, G. H. Gelinck, R. Resel, D. M. de Leeuw and P. Strohriegl, *Adv. Funct. Mater.*, 2013, **23**, 2016.
7 H. Langhals, *Helv. Chim. Acta*, 2005, **88**, 1309.
8 M. A. Muth, G. Gupta, A. Wicklein, M. Carrasco-Orozco, T. Thurn-Albrecht and M. Thelakkat, *J. Phys. Chem. C*, 2014, **118**, 92.
9 T. J. Zhang, D. M. Sun, X. K. Ren, L. L. Liu, G. Y. Wen, Z. J. Ren, H. H. Li and S. K. Yan, *Soft Matter*, 2013, **9**, 10739.
10 L. Wang, L. Xu, K. G. Neoh and E.-T. Kang, *J. Mater. Chem.*, 2011, **21**, 6502.
11 F. Yukruk, A. L. Dogan, H. Canpinar, D. Guc and E. U. Akkaya, *Org. Lett.*, 2005, **7**, 2885.
12 M. Z. Yin, J. Shen, R. Gropeanu, G. O. Pflugfelder, T. Weil and K. Mullen, *Small*, 2008, **4**, 894.
13 M. Yin, J. Shen, G. O. Pflugfelder and K. Mullen, *J. Am. Chem. Soc.*, 2008, **130**, 7806.
14 C. Kohl, T. Weil, J. Q. Qu and K. Mullen, *Chem. – Eur. J.*, 2004, **10**, 5297.

15 S. K. Yang, X. H. Shi, S. Park, S. Doganay, T. Ha and S. C. Zimmerman, *J. Am. Chem. Soc.*, 2011, **133**, 13206.
16 Z. G. Zhang, C. L. Zhan, X. Zhang, S. L. Zhang, J. H. Huang, A. D. Q. Li and J. N. Yao, *Chem. – Eur. J.*, 2012, **18**, 12305.
17 S. Rehm, V. Stepanenko, X. Zhang, T. H. Rehm and F. Wurthner, *Chem. – Eur. J.*, 2010, **16**, 3372.
18 H. Langhals, W. Jona, F. Einsiedl and S. Wohnlich, *Adv. Mater.*, 1998, **10**, 1022.
19 Y. Liu, K. R. Wang, D. S. Guo and B. P. Jiang, *Adv. Funct. Mater.*, 2009, **19**, 2230.
20 T. Heek, C. Fasting, C. Rest, X. Zhang, F. Wurthner and R. Haag, *Chem. Commun.*, 2010, **46**, 1884.
21 B. X. Gao, H. X. Li, H. M. Liu, L. C. Zhang, Q. Q. Bai and X. W. Ba, *Chem. Commun.*, 2011, **47**, 3894.
22 U. Hahn, S. Engmann, C. Oelsner, C. Ehli, D. M. Guldi and T. Torres, *J. Am. Chem. Soc.*, 2010, **132**, 6392.
23 K.-R. Wang, H.-W. An, F. Qian, Y.-Q. Wang, J.-C. Zhang and X.-L. Li, *RSC Adv.*, 2013, **3**, 23190.
24 M. A. Abdalla, J. Bayer, J. O. Radler and K. Mullen, *Angew. Chem., Int. Ed.*, 2004, **43**, 3967.
25 J. K. Gallaher, E. J. Aitken, R. A. Keyzers and J. M. Hodgkiss, *Chem. Commun.*, 2012, **48**, 7961.
26 J. Schonamsgruber, B. Schade, R. Kirschbaum, J. Li, W. Bauer, C. Bottcher, T. Drewello and A. Hirsch, *Eur. J. Org. Chem.*, 2012, 6179.
27 C. D. Schmidt, C. Boettcher and A. Hirsch, *Eur. J. Org. Chem.*, 2007, 5497.
28 C. D. Schmidt, C. Bottcher and A. Hirsch, *Eur. J. Org. Chem.*, 2009, 5337.
29 C. Backes, C. D. Schmidt, K. Rosenlehner, F. Hauke, J. N. Coleman and A. Hirsch, *Adv. Mater.*, 2010, **22**, 788.
30 J. M. Englert, J. Rohrl, C. D. Schmidt, R. Graupner, M. Hundhausen, F. Hauke and A. Hirsch, *Adv. Mater.*, 2009, **21**, 4265.
31 N. V. Kozhemyakina, J. M. Englert, G. A. Yang, E. Spiecker, C. D. Schmidt, F. Hauke and A. Hirsch, *Adv. Mater.*, 2010, **22**, 5483.
32 H. Yang, Y. Hernandez, A. Schlierf, A. Felten, A. Eckmann, S. Johal, P. Louette, J. J. Pireaux, X. Feng, K. Mullen, V. Palermo and C. Casiraghi, *Carbon*, 2013, **53**, 357.
33 D. Magde, R. Wong and P. G. Seybold, *Photochem. Photobiol.*, 2002, **75**, 327.
34 C. Huang, S. Barlow and S. R. Marder, *J. Org. Chem.*, 2011, **76**, 2386.
35 A. D. Q. Li, W. Wang and L. Q. Wang, *Chem. – Eur. J.*, 2003, **9**, 4594.
36 X. W. Yu, C. L. Zhan, X. L. Ding, S. L. Zhang, X. Zhang, H. Y. Liu, L. L. Chen, Y. S. Wu, H. B. Fu, S. G. He, Y. Huang and J. N. Yao, *Phys. Chem. Chem. Phys.*, 2013, **15**, 11960.
37 A. Bossi and P. G. Righetti, *Electrophoresis*, 1997, **18**, 2012.
38 D. Gorl, X. Zhang and F. Wurthner, *Angew. Chem., Int. Ed.*, 2012, **51**, 6328.
39 W. E. Ford, *J. Photochem.*, 1987, **37**, 189.
40 R. Greenwood and K. Kendall, *J. Eur. Ceram. Soc.*, 1999, **19**, 479.
41 H. Langhals and W. Jona, *Chem. – Eur. J.*, 1998, **4**, 2110.
42 G. Turkmen, S. Erten-Ela and S. Icli, *Dyes Pigm.*, 2009, **83**, 297.
43 L. Zang, R. C. Liu, M. W. Holman, K. T. Nguyen and D. M. Adams, *J. Am. Chem. Soc.*, 2002, **124**, 10640.
44 A. P. de Silva, T. S. Moody and G. D. Wright, *Analyst*, 2009, **134**, 2385.
45 R. A. Bissell, A. P. De Silva, H. Q. N. Gunaratne, P. L. M. Lynch, G. E. M. Maguire and K. R. A. S. Sandanayake, *Chem. Soc. Rev.*, 1992, **21**, 187.
46 A. P. de Silva, *J. Phys. Chem. Lett.*, 2011, **2**, 2865.
47 R. A. Bissell, A. P. de Silva, H. Q. N. Gunaratne, P. L. M. Lynch, G. E. M. Maguire, C. P. McCoy and K. R. A. S. Sandanayake, *Top. Curr. Chem.*, 1993, **168**, 223.
48 L. M. Daffy, A. P. de Silva, H. Q. N. Gunaratne, C. Huber, P. L. M. Lynch, T. Werner and O. S. Wolfbeis, *Chem. – Eur. J.*, 1998, **4**, 1810.
49 N. I. Georgiev, A. R. Sakr and V. B. Bojinov, *Dyes Pigm.*, 2011, **91**, 332.
50 H. N. Lee, Z. C. Xu, S. K. Kim, K. M. K. Swamy, Y. Kim, S. J. Kim and J. Yoon, *J. Am. Chem. Soc.*, 2007, **129**, 3828.
51 H. Tian, J. Gan, K. C. Chen, J. He, Q. L. Song and X. Y. Hou, *J. Mater. Chem.*, 2002, **12**, 1262.
52 X. R. He, H. B. Liu, Y. L. Li, S. Wang, Y. J. Li, N. Wang, J. C. Xiao, X. H. Xu and D. B. Zhu, *Adv. Mater.*, 2005, **17**, 2811.
53 X. J. Liu, N. Zhang, J. Zhou, T. J. Chang, C. L. Fang and D. H. Shangguan, *Analyst*, 2013, **138**, 901.
54 K. Peneva, G. Mihov, A. Herrmann, N. Zarrabi, M. Borsch, T. M. Duncan and K. Mullen, *J. Am. Chem. Soc.*, 2008, **130**, 5398.
55 K. Qvortrup, A. D. Bond, A. Nielsen, C. J. McKenzie, K. Kilsa and M. B. Nielsen, *Chem. Commun.*, 2008, 1986.
56 H. X. Wang, D. L. Wang, Q. Wang, X. Y. Li and C. A. Schalley, *Org. Biomol. Chem.*, 2010, **8**, 1017.
57 M. T. Vagnini, A. L. Smeigh, J. D. Blakemore, S. W. Eaton, N. D. Schley, F. D'Souza, R. H. Crabtree, G. W. Brudvig, D. T. Co and M. R. Wasielewski, *Proc. Natl. Acad. Sci. U. S. A.*, 2012, **109**, 15651.
58 B. Roy, T. Noguchi, D. Yoshihara, Y. Tsuchiya, A. Dawn and S. Shinkai, *Org. Biomol. Chem.*, 2013, **12**, 561.
59 Y. Che, X. M. Yang and L. Zang, *Chem. Commun.*, 2008, 1413.
60 V. Stepanenko, M. Stocker, P. Muller, M. Buchner and F. Wurthner, *J. Mater. Chem.*, 2009, **19**, 6816.
61 V. Stepanenko and F. Wurthner, *Small*, 2008, **4**, 2158.
62 F. Wurthner and A. Sautter, *Org. Biomol. Chem.*, 2003, **1**, 240.
63 F. Wurthner, C. C. You and C. R. Saha-Moller, *Chem. Soc. Rev.*, 2004, **33**, 133.
64 C. C. You and F. Wurthner, *J. Am. Chem. Soc.*, 2003, **125**, 9716.
65 P. J. Stang and B. Olenyuk, *Acc. Chem. Res.*, 1997, **30**, 502.
66 C. Piguet, M. Borkovec, J. Hamacek and K. Zeckert, *Coord. Chem. Rev.*, 2005, **249**, 705.
67 L. Brunsveld, B. J. B. Folmer, E. W. Meijer and R. P. Sijbesma, *Chem. Rev.*, 2001, **101**, 4071.

68 L. Fabbrizzi, M. Licchelli, P. Pallavicini, D. Sacchi and A. Taglietti, *Analyst*, 1996, **121**, 1763.
69 G. DeSantis, L. Fabbrizzi, M. Licchelli, A. Poggi and A. Taglietti, *Angew. Chem., Int. Ed.*, 1996, **35**, 202.
70 F. Würthner, C. Thalacker, S. Diele and C. Tschierske, *Chem. – Eur. J.*, 2001, **7**, 2245.
71 A. Arnaud, J. Belleney, F. Boue, L. Bouteiller, G. Carrot and W. Wintgens, *Angew. Chem., Int. Ed.*, 2004, **43**, 1718.
72 K. Balakrishnan, A. Datar, T. Naddo, J. L. Huang, R. Oitker, M. Yen, J. C. Zhao and L. Zang, *J. Am. Chem. Soc.*, 2006, **128**, 7390.
73 F. Wurthner, Z. Chen, V. Dehm and V. Stepanenko, *Chem. Commun.*, 2006, 1188.
74 B. Bodenant, F. Fages and M. H. Delville, *J. Am. Chem. Soc.*, 1998, **120**, 7511.
75 S. Yagai, Y. Monma, N. Kawauchi, T. Karatsu and A. Kitamura, *Org. Lett.*, 2007, **9**, 1137.
76 W. Wang, J. J. Han, L. Q. Wang, L. S. Li, W. J. Shaw and A. D. Q. Li, *Nano Lett.*, 2003, **3**, 455.
77 W. Wang, L. S. Li, G. Helms, H. H. Zhou and A. D. Q. Li, *J. Am. Chem. Soc.*, 2003, **125**, 1120.
78 W. Wang, W. Wan, H. H. Zhou, S. Q. Niu and A. D. Q. Li, *J. Am. Chem. Soc.*, 2003, **125**, 5248.
79 E. E. Neuteboom, S. C. J. Meskers, E. W. Meijer and R. A. J. Janssen, *Macromol. Chem. Phys.*, 2004, **205**, 217.
80 Z. J. Chen, V. Stepanenko, V. Dehm, P. Prins, L. D. A. Siebbeles, J. Seibt, P. Marquetand, V. Engel and F. Würthner, *Chem. – Eur. J.*, 2007, **13**, 436.
81 T. Heek, F. Würthner and R. Haag, *Chem. – Eur. J.*, 2013, **19**, 10911.
82 A. Datar, K. Balakrishnan and L. Zang, *Chem. Commun.*, 2013, **49**, 6894.
83 M. R. Harpham, N. E. Levinger and B. M. Ladanyi, *J. Phys. Chem. B*, 2008, **112**, 283.
84 D. B. Wong, K. P. Sokolowsky, M. I. El-Barghouthi, E. E. Fenn, C. H. Giammanco, A. L. Sturlaugson and M. D. Fayer, *J. Phys. Chem. B*, 2012, **116**, 5479.
85 J. Catalan, C. Diaz and F. Garcia-Blanco, *J. Org. Chem.*, 2001, **66**, 5846.
86 A. Luzar, *J. Mol. Liq.*, 1990, **46**, 221.
87 B. Kirchner and M. Reiher, *J. Am. Chem. Soc.*, 2002, **124**, 6206.
88 B. K. Miremadi and S. R. Morrison, *J. Appl. Phys.*, 1988, **63**, 4970.
89 L. A. Xue, N. Ranjan and D. P. Arya, *Biochem.*, 2011, **50**, 2838.

